

---

# FORMULATIONS FOR COPRODUCT LIGNIN-BASED PLASTICS

---

## Authors

---

Simo Sarkanen

---

Yi-ru Chen

---

Yun-Yan Wang

## ORGANIZATION

---



University of Minnesota

---



University of Minnesota

---



University of Minnesota

# TABLE OF CONTENTS

LIST OF FIGURES.....	3
LIST OF TABLES.....	3
LIST OF ACRONYMS .....	3
EXECUTIVE SUMMARY.....	4
INTRODUCTION .....	5
TASK 1: PLASTICIZERS FOR LIGNIN-BASED POLYMERIC MATERIALS.....	6
TASK 2: FUNCTIONAL POLYMERIC MATERIALS BASED ON NARA LIGNINSULFONATES.....	7
TASK 3: TECHNO-ECONOMIC ANALYSIS OF NARA LS-BASED POLYMERIC MATERIALS.....	11
NARA OUTPUTS .....	17
NARA OUTCOMES .....	18
FUTURE DEVELOPMENT .....	18
LIST OF REFERENCES .....	19

[nararenewables.org](http://nararenewables.org)  BY-NC-ND



NARA is led by Washington State University and supported by the Agriculture and Food Research Initiative Competitive Grant no. 2011-68005-30416 from the USDA National Institute of Food and Agriculture.



Any opinions, findings, conclusions, or recommendations expressed in this publication are those of the author(s) and do not necessarily reflect the view of the U.S. Department of Agriculture.

# LIST OF FIGURES

FIGURE NO.	FIGURE TITLE	PAGE NO.
LBP-1.1.	Tensile behavior of polymeric materials based on unmethylated and methylated ball-milled softwood lignin .....6	6
LBP-2.1.	Relationship between tensile strength ( $\sigma_{max}$ ) and elongation-at-break ( $\Delta\epsilon$ %) for FS-10 ligninsulfonate-based polymeric materials alone and in blends with miscible components .....7	7
LBP-2.2.	Tensile behavior of polymeric materials composed of unmethylated FS-01 ligninsulfonate (LS) blended with aliphatic polyesters .....8	8
LBP-2.3.	Tensile behavior of polymeric materials based on unmethylated ligninsulfonates with different molecular weights .....8	8
LBP-2.4.	Tensile behavior of LS-based and sMLS-based polymeric materials unblended and blended with 15 wt% PTMG .....9	9
LBP-2.5.	X-ray powder diffraction patterns of uncast and cast polymeric materials based on unmethylated and methylated ligninsulfonates .....9	9
LBP-2.6.	Packing of macromolecular entities in ligninsulfonate (LS)-based polymeric materials cast at 115° and then 150°C .....10	10
LBP-3.1.	A schematic process flow for producing lignosulfonate-based polymeric materials .....11	11
LBP-3.2.	Cumulative cash flow diagram for discounted after-tax cash flows as a function of H-LS selling price when $FCI_L$ = Grass Roots Cost in Table LBP-3.2 .....15	15
LBP-3.3.	Cumulative cash flow diagram for discounted after-tax cash flows as a function of H-LS selling price when $FCI_L$ = Total Module Cost in Table LBP-3.2 .....15	15
LBP-3.4.	Cumulative cash flow diagram for discounted after-tax cash flows as a function of H-LS selling price when $FCI_L$ = 20% of Grass Roots Cost in Table LBP-3.2 .....16	16

# LIST OF TABLES

TABLE NO.	TABLE TITLE	PAGE NO.
LBP-3.1.	Bare module cost for equipment estimated by CAPCOST computer program .....12	12
LBP-3.2.	The annual utility cost estimated by CAPCOST .....12	12
LBP-3.3.	Cost of Materials estimated by CAPCOST .....13	13
LBP-3.4.	Estimation of cost of manufacturing without depreciation (COMd) by CAPCOST .....14	14
LBP-3.5.	Net present value, return rate and payback period for project as a function of H-LS selling price when $FCI_L$ = Grass Roots Cost in Table LBP-3.2 .....15	15
LBP-3.6.	Net present value, return rate and payback period for project as a function of H-LS selling price when $FCI_L$ = Total Module Cost in Table LBP-3.2 .....15	15
LBP-3.7.	Net present value, return rate and payback period for project as a function of H-LS selling price when $FCI_L$ = 20% of Grass Roots Cost in Table LBP-3.2 .....16	16
LBP-3.8.	The selling price of lignosulfonate-based blends containing 15% polyester and polyols. The market price for blend components was assessed at \$2.60-3.26/kg in 2014 .....16	16

# LIST OF ACRONYMS

BML	ball-milled lignin
dMLS	ligninsulfonate methylated with dimethyl sulfate followed by diazomethane
DMSO	dimethyl sulfoxide
LS	ligninsulfonate
sMLS	ligninsulfonate methylated with dimethyl sulfate alone

# EXECUTIVE SUMMARY

Since the 1970's, efforts to create lignin-based plastics have been guided by a mistaken notion (first developed over half-a-century ago) that lignins are crosslinked. Consequently, it has been difficult to overcome a 40 wt% incorporation limit for lignin derivatives in functional polymeric materials. Rather than being crosslinked, however, constituent lignin species are associated macromolecular complexes that are held together by strong intermolecular forces between the individual components. Thus, the creation of continuity between adjoining complexes in the polymeric materials becomes a central issue. We have demonstrated that polymeric blends containing 85–100 wt% Jack pine ball-milled lignin and its methylated derivative can be converted into plastics with mechanical properties that compare very favorably with common commodity plastics. These findings have guided us to successfully reach the goal of converting NARA

coproduct ligninsulfonates (LS) into functional polymer blends with high (85–100 wt%) ligninsulfonate contents. For example, underivatized NARA LS-based blends containing 15 wt% poly(trimethylene glutarate), a commercially available aliphatic polyester, possess the same tensile strength as polystyrene (46 MPa), but with a 3-fold greater elongation-at-break. The corresponding blends with methylated LS exhibit an elongation-at-break that has increased by another 50%. The mechanical properties of these novel biodegradable LS-based polymeric materials can be effectively modulated by blend components. These results are truly paradigm-shifting in the field of lignin-based plastics. Once the blend formulations are optimized, techno-economic analysis shows that the polymeric materials with 85–100 wt% LS contents would be feasible options for replacing polystyrene as alternative sources of engineering plastics.

# INTRODUCTION

The scale of biofuels production from lignocellulosic biomass to be implemented by 2030 (U.S. DOE 2006) will give rise to more than 200 million tons of lignin derivatives annually. As the efficiency of lignocellulose saccharification and fermentation improves, less lignin will be needed as solid fuel to produce heat for biorefinery operations. A reliable basis must be developed for converting coproduct lignins into functional thermoplastics and other useful polymeric materials. The overall US annual production of polystyrene is 14 million tons. General purpose polystyrene was traded at around \$1,590/ton cost and freight from China in the Asian market in May 2011 (<http://www.icis.com/resources/news/2007/11/06/9076435/polystyrene-ps-prices-and-pricing-information/>). Therefore, the NARA ligninsulfonate obtained from the SPORL (Zhu *et al.* 2015) process could be viewed an attractive resource for producing future sustainable polymeric materials, and in return, improve the economic viability of the SPORL process to a significant extent.

Much of the preceding forty-year quest for lignin-based plastics has been hindered by a fundamental misperception of lignin macromolecules as “three-dimensionally branched network” polymers (Hsu & Glasser 1976). High lignin contents were thought to generate a profusion of hard segments in rigid polymeric materials that would be of limited usefulness. Thus, substantial levels of soft segments (introduced by chemical reaction or by blending) were considered to be a necessary feature of lignin-containing formulations that stood a chance of competing with traditional polymeric-material commodities from petrochemical sources. Such a view has persisted in some quarters until the present time (Saito *et al.*, 2012), and a recent application of the concept in producing lignin–polybutadiene polyurethanes

(embodying 65–75 wt% hardwood lignin contents) resulted in tensile strengths extending to ~4 MPa with elongations at break reaching ~15% (Saito *et al.*, 2013). The relationships observed between the tensile behavior and composition of the polymeric materials were promising (in regard to their adjustability), but a 10-fold greater tensile strength would have been more encouraging.

This exemplifies a result of the erroneous supposition that the hydrodynamic compactness of lignin polymer chains arise from crosslinking (Chen & Sarkanen, 2006). During the past six years, however, it has become evident that the intermolecular attraction between pairs of interacting aromatic rings in lignin components is remarkably strong, leading to 7–11 kcal/mol stabilization energies in each case (Chen & Sarkanen, 2010). The consequences for lignin preparations and their simple derivatives are profound. The majority of the constituent components are incorporated into huge supramacromolecular complexes that are largely responsible for the notorious brittleness of lignin-based materials (Chen & Sarkanen, 2006).

In recognizing that polymeric lignin preparations are actually composed of associated complexes, it has become possible to create functional materials from simple lignin derivatives alone. Indeed, these utterly new lignin-based materials can surpass polystyrene in mechanical properties. Such findings have been achieved with Jack pine ball-milled lignins (BML). We have successfully extended the knowledge gained from BML-based polymeric materials to formulations based on high levels (85–100 wt%) of NARA ligninsulfonate preparations (Wang *et al.*, 2015).

# TASK 1: PLASTICIZERS FOR LIGNIN-BASED POLYMERIC MATERIALS

## Objective

Prior to embarking on a wide-ranging search for effective plasticizers for NARA Douglas-fir LS-based polymeric materials, a reference point was created through a preliminary investigation of softwood (native) lignin-based plastics. Thus, our studies were first dedicated to milled wood lignins that have traditionally been considered to represent structural averages of native lignins in softwood cell walls. The blend components that resulted in these lignin-based plastics, with very promising mechanical properties, provided the focus of attention in the development of NARA LS-based polymeric materials. Moreover, in an effort to access potential industrial applications, the question of whether the starting ligninsulfonate preparations should be methylated has been a central issue in our studies. Comparison of the tensile properties of the underivatized and methylated ball-milled Jack lignin-based materials could provide valuable insight in the quest for unmethylated NARA LS-based polymeric materials.

## Methodology

A native softwood ball-milled lignin (BML) was isolated by extracting Jack pine wood meal with aqueous 96% dioxane in the traditional manner. Without fractionation, this parent BML sample was methylated with dimethyl sulfate in alkaline solution and then with diazomethane in chloroform, as previously described for softwood kraft lignins (Li & Sarkanen, 2002, 2005). Formulations were developed for functional plastics containing 85–100 wt% levels BML or its methylated derivatives. Cheap commercially-available miscible blend components were given the most attention. After solution-casting in DMSO, the mechanical properties were characterized through tensile tests with an Instron 5542 apparatus equipped with grips to which serrated faces had been attached. Insight into the arrangements of the aromatic rings in the constituent macromolecular lignin complexes were obtained through X-ray powder diffraction studies.

## Results

The unmethylated ball-milled lignin (BML)-based material was about 20% weaker than its methylated counterpart, but blending with 5 wt% tetrabromobisphenol A (a flame retardant) resulted in a 60% improvement in tensile strength (Figure LBP-1.1). A typical methylated (native) ball-milled softwood lignin (Mw 3400) can be converted into a polymeric material that manifests better tensile behavior than polystyrene. In the presence of 5–15 wt% miscible blend components, the resulting polymeric materials can approach 70 MPa in tensile strength as elongation-at-break reaches 10% (Figure LBP-1.1). Few polymeric materials in common use can

exceed these lignin-based plastics in engineering stress, and thus the frontier of next-generation applications for co-product lignins has been reached.

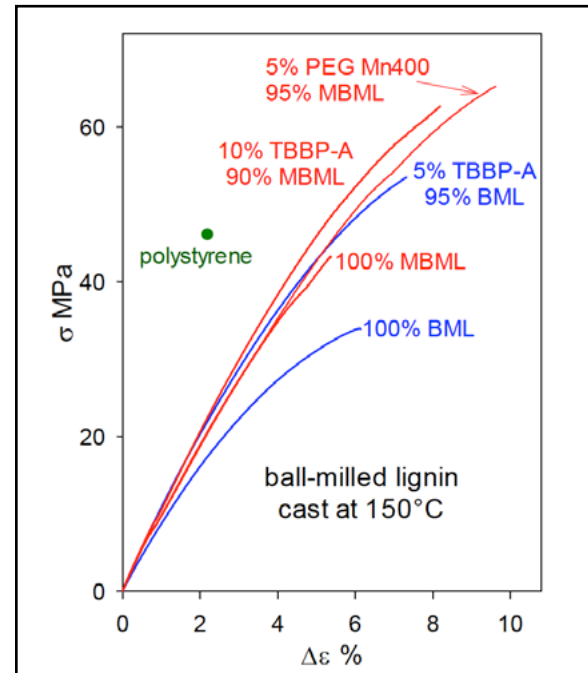


Figure LBP-1.1: Tensile behavior of polymeric materials based on unmethylated and methylated ball-milled softwood lignin. BML: ball-milled softwood lignin; MBML: methylated ball-milled lignin; TBBP-A: tetrabromobisphenol A. PEG: poly(ethylene glycol),  $M_n$  400.

## Conclusions

In recognizing that macromolecular lignin species are associated complexes rather than crosslinked entities, we have taken an entirely new approach to developing lignin-based plastics. Consequently, we have documented that methylated BML alone could be converted into plastics with mechanical properties that compare very favorably to polystyrene. On the other hand, formulations composed of underivatized BML and 5–15 wt% commercially available blend components yield materials with tensile properties surpassing those of polystyrene. This is a centrally important step in developing NARA LS-based polymeric materials with potential for industrial applications.

# TASK 2: FUNCTIONAL POLYMERIC MATERIALS BASED ON NARA LIGNINSULFONATES

## Objective

We have successfully developed promising formulations for converting Jack pine BML into plastics with the highest attainable lignin contents. These unprecedented achievements have paved the way for converting NARA ligninsulfonates (LS) into useful polymeric materials with mechanical properties approaching those of polystyrene (46 MPa strength, 2% elongation-at-break). A positive outcome will enable productive communication with the private sector to explore translation from laboratory practice to industrial applications. This will greatly improve the economic viability of NARA's platform in converting post-harvest forest residuals (e.g., Douglas-fir) into biojet fuel.

## Methodology

Two batches (FS-10 and FS-01) of spent liquor have been provided by Dr. Junyong (JY) Zhu from calcium bisulfite pretreatment of Douglas-fir. Both batches were subjected to consecutive ultrafiltration through 200 kDa and 4 kDa nominal-molecular-weight cutoff membranes. The  $M_w$  and polydispersity index of FS-10 LS were 9,600 and 5.0, respectively, while those of FS-01 were 7,100 and 3.8. Polymeric materials were produced (by DMSO-solution casting) from the underivatized LS as well as from the derivatives formed by methylation with dimethyl sulfate alone (sMLS) and (separately) with dimethyl sulfate followed by diazomethane (dMLS) with or without additional blend components. Candidate blend components were chosen on the basis of the promising plastics formulations composed of BML. The effects of molecular weight were examined in terms of mechanical behavior of the resulting LS-based plastics. Casting conditions were adjusted so as to ensure complete solvent removal. X-ray powder diffraction was used to gain information about the inner and peripheral domains in the constituent associated lignin complexes. Atomic force microscopy was employed to estimate the effective dimensions of these associated macromolecular entities in the LS-based polymeric materials.

## Results

Unmethylated FS-10 LS samples ( $M_w$  9,600, polydispersity index 5.0) blended individually with 10 wt% poly(ethylene glycol) or various aliphatic polyesters at 15 wt% levels exhibited a range of tensile behavior that could match polyethylene (30 MPa, 9% elongation-at-break). These results embody a trend that, through suitably extended blend formulations, should be capable of approaching the tensile strength of polystyrene (Figure LBP-2.1). Phenolic-hydroxyl-group methylation of the FS-10 LS only results in a small improvement in the tensile strength of the resulting sMLS (Figure LBP-2.1).

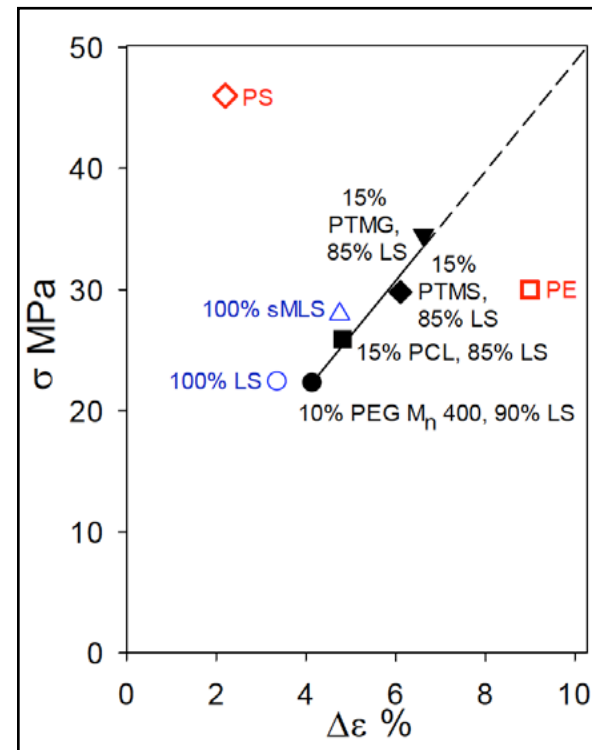


Figure LBP-2.1. Relationship between tensile strength ( $\sigma_{max}$ ) and elongation-at-break ( $\Delta\epsilon$  %) for FS-10 ligninsulfonate-based polymeric materials alone and in blends with miscible components: LS: ligninsulfonate; PEG: poly(ethylene glycol); PTMG: poly(trimethylene glutarate); PTMS: poly(trimethylene succinate); sMLS: ligninsulfonate methylated with dimethyl sulfate; PE: polyethylene; PS: polystyrene.

As far as FS-01 is concerned, with both the  $M_w$  and polydispersity index being ~1.3-fold smaller than the corresponding parameters for the FS-10 sample, it became possible to achieve 40 MPa tensile strengths with blends containing 15 wt% levels of at least two different aliphatic polyesters, namely, poly(ethylene malonate) and poly(ethylene succinate) (Figure LBP-2.2). These materials are 13% weaker than polystyrene but 30% stronger than polyethylene in their tensile behavior. Thus, ligninsulfonate-based polymeric materials show considerable promise in being able to surpass polystyrene in mechanical properties.

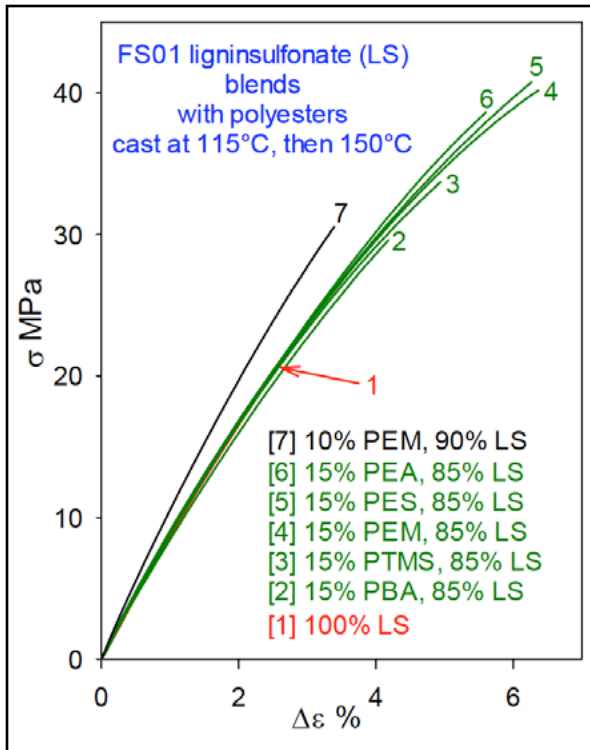


Figure LBP-2.2. Tensile behavior of polymeric materials composed of unmethylated FS-01 ligninsulfonate (LS) blended with aliphatic polyesters. PBA: poly(butylene adipate); PEA: poly(ethylene adipate); PEM: poly(ethylene malonate); PES: poly(ethylene succinate); PTMS: poly(trimethylene succinate). FS-01 LS  $M_w = 7100$ ,  $M_w/M_n = 3.8$ .

The effects of molecular weight and blend components in these novel NARA FS-sample formulations are exemplified by a comparison of the tensile behavior of polymeric materials based on unmethylated FS-10 ( $M_w$  9600,  $M_w/M_n = 5.0$ ) and FS-01 ( $M_w$  7100,  $M_w/M_n = 3.8$ ) LS preparations (Figure LBP-2.3). Polymeric materials composed solely of FS-01 are weaker than those produced from FS-10. However, FS-01-based blends containing 15 wt% poly(trimethylene glutarate) possess the same tensile strength as polystyrene, but with a much greater elongation-at-break. With the same formulation, methylating FS-01 with dimethyl sulfate alone increases the elongation-at-break by 50% (Figure LBP-2.4).

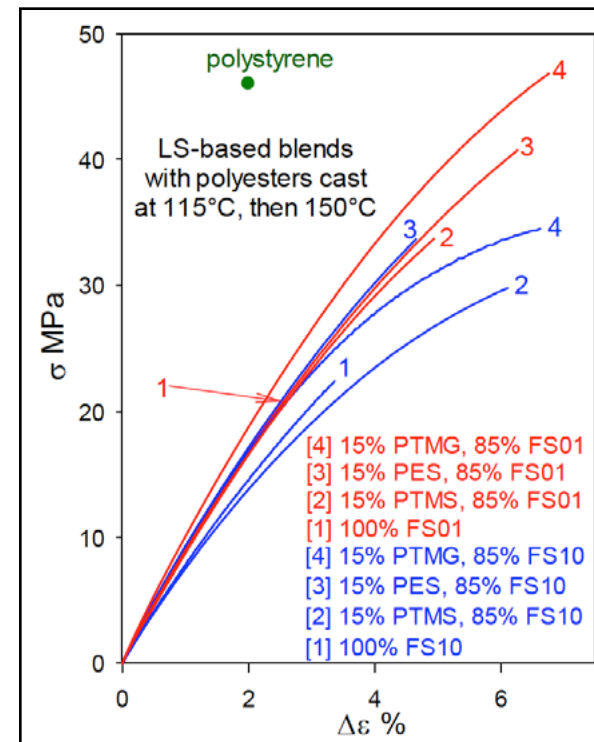


Figure LBP-2.3. Tensile behavior of polymeric materials based on unmethylated ligninsulfonates with different molecular weights. PES: poly(ethylene succinate); PTMG: poly(trimethylene glutarate); PTMS: poly(trimethylene succinate). FS-10 LS  $M_w = 9600$ ,  $M_w/M_n = 5$ ; FS-01 LS  $M_w = 7100$ ,  $M_w/M_n = 3.8$ .

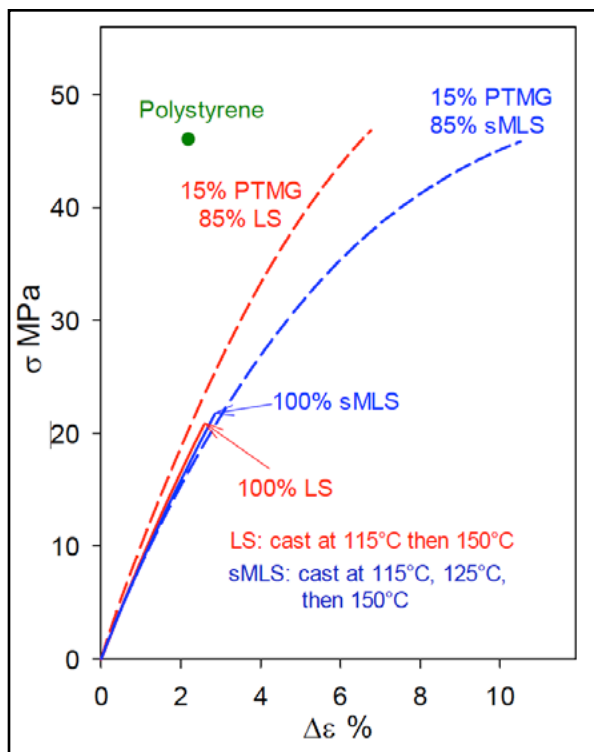


Figure LBP-2.4. Tensile behavior of LS-based and sMLS-based polymeric materials unblended and blended with 15 wt% PTMG. Both blends surpass polystyrene decisively. LS: FS-01 unmethylated ligninsulfonate; sMLS: FS-01 ligninsulfonate methylated only with dimethyl sulfate; PTMG: poly(trimethylene glutarate).

X-ray powder diffraction studies revealed that, like BML-based plastics, these novel NARA LS-based polymeric materials are assembled from macromolecular species that interact with one another in such a way as to prevent latent Å- or nm-scale voids from appearing between neighboring entities. The inner regions of the macromolecular species are primarily occupied by cofacial arrangements of interacting aromatic rings which are more stable. On the other hand, the less stable edge-on orientations are more frequent among the peripheral chain segments. In the cast materials, the need for continuity between adjoining macromolecular entities determines the relative proportions of the cofacial and edge-on interacting-aromatic-ring domains (Figure LBP-2.5). It is the peripheral region that interacts preferentially with non-lignin blend components.

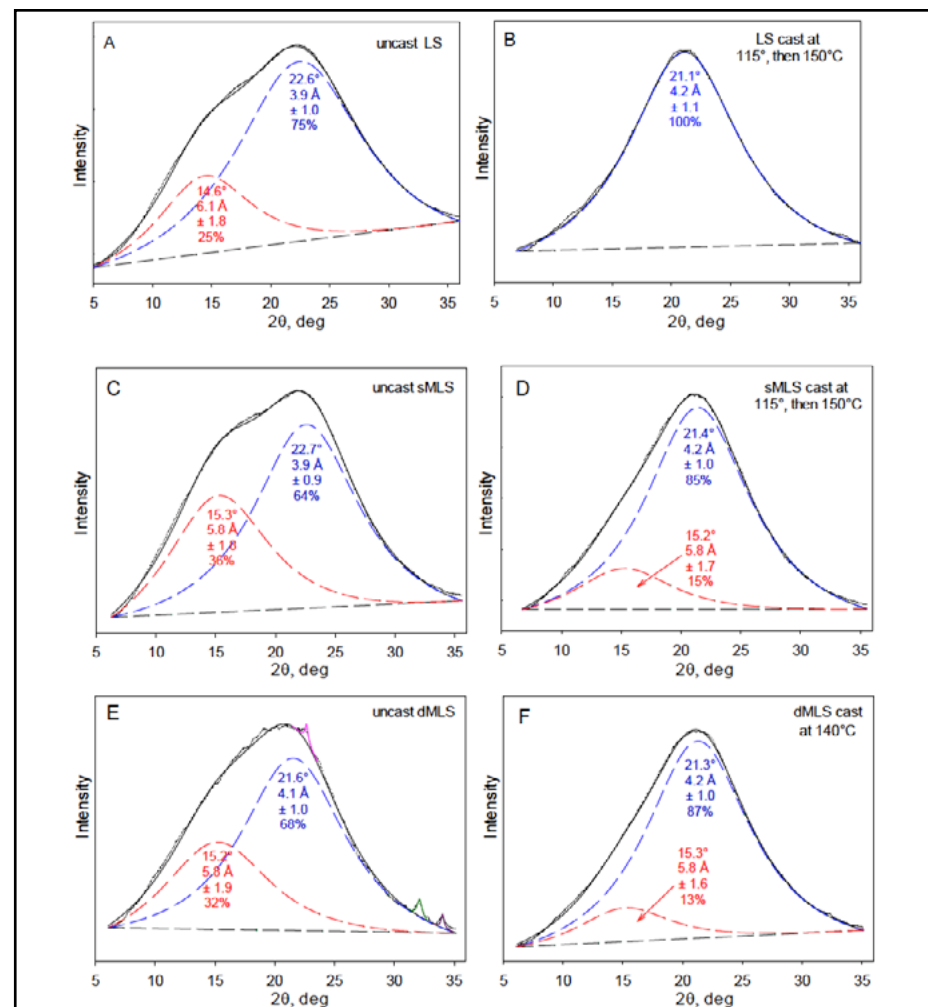


Figure LBP-2.5. X-ray powder diffraction patterns of uncast and cast polymeric materials based on unmethylated and methylated ligninsulfonates. (A) uncast and (B) cast unmethylated ligninsulfonate (LS); (C) uncast and (D) cast ligninsulfonate methylated with dimethyl sulfate (sMLS); (E) uncast and (F) cast ligninsulfonate successively methylated with dimethyl sulfate and diazomethane (dMLS). The x-ray diffraction patterns of the amorphous polymeric materials were analyzed by fitting two Lorentzian functions  $I(x) = I(0)/(1 + x^2/hwhm^2)$ ,  $x = 2\theta - 2\theta_0$ , where  $I(x)$  is the scattered intensity at  $x$  from the Bragg angle  $2\theta_0$  for the peak,  $2\theta_0$  is the scattering angle, and  $hwhm$  is the half-width at the half-maximum of the peak.

Atomic force microscopy revealed that the effective dimensional ranges of the associated macromolecular entities in the three cast ligninsulfonate (LS)-based polymeric materials are  $12.2 \pm 3.2$ ,  $16.7 \pm 4.3$  and  $20.3 \pm 5.5$  nm, respectively for the underivatized, sMLS and dMLS preparations. The amplitude images of the three ultramicrotomed material surfaces are depicted in Figures LBP-2.6 A–C. For confirmatory purposes, a corresponding height image is exemplified in Figure LBP-2.6 D. The increase in diameter of these macromolecular species is likely to

result from coalescence during casting because methylation is not expected to cause covalent formation of larger entities. The likelihood of coalescence rests on the molecular-weight dependence of the intermolecular interactions between the individual LS components. In this respect, it seems that the macromolecular entities in the cast sMLS- and dMLS-based materials are (in three dimensions) 2.17- and 3.98-fold larger, respectively, than those making up the unmethylated LS. Such a situation could occur, for example, if the strongest noncovalent interactions between the methylated LS components were to involve the intermediate rather than higher chain lengths.

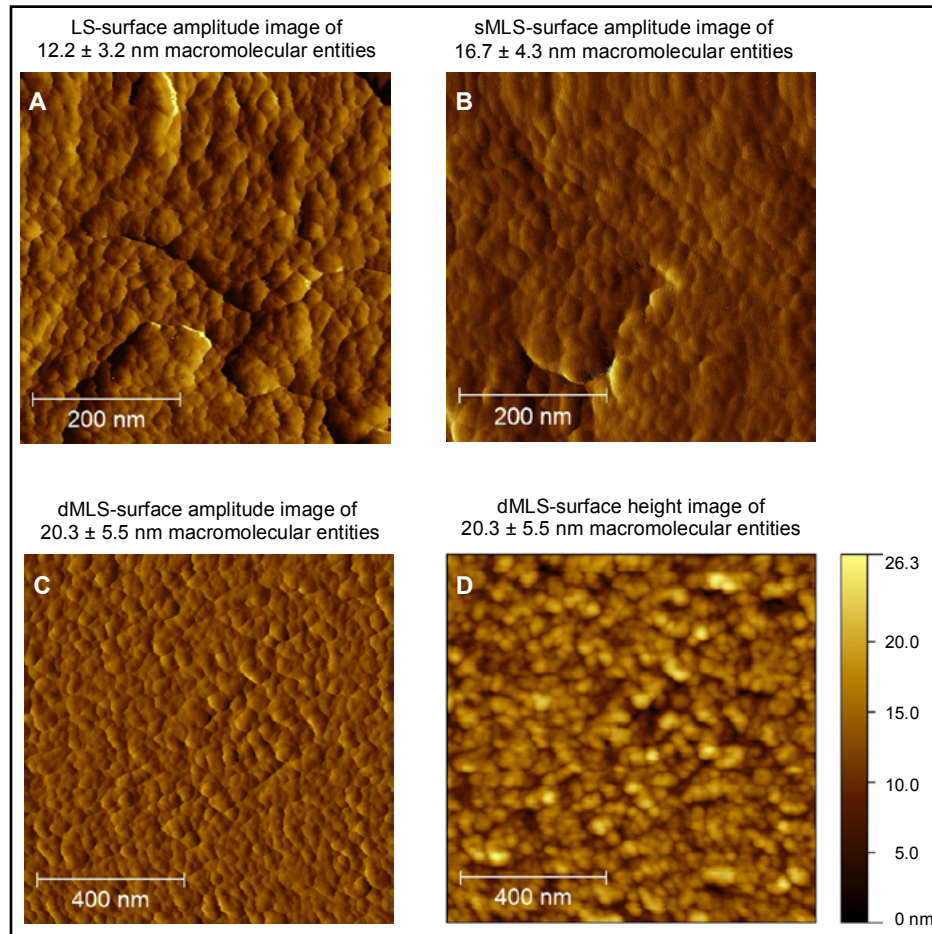


Figure LBP-2.6. Packing of macromolecular entities in ligninsulfonate (LS)-based polymeric materials cast at 115° and then 150°C. Tapping-mode AFM amplitude images of ultramicrotome-cut surfaces of (A) unmethylated LS, (B) LS methylated with dimethyl sulfate (sMLS), (C) LS successively methylated with dimethyl sulfate and diazomethane (dMLS); (D) corresponding height image of dMLS surface (material cast stepwise at 115°, 125° and 150°C).

## Conclusions

The mechanical properties of LS-based polymeric materials were strongly influenced by the molecular weight distributions of the starting materials. The tensile behavior of polymeric materials containing simple softwood LS at 85–100 wt% levels can surpass unplasticized polystyrene. Certain commercially available aliphatic polyesters (such as poly(trimethylene glutarate)) can be effective plasticizers for ligninsulfonate-based plastics. Systematic approaches should be devised to identify plasticizers for developing functional polymeric materials with highest attainable underivatized ligninsulfonate contents. This will greatly increase the likelihood of industrial applications.

# TASK 3: TECHNO-ECONOMIC ANALYSIS OF NARA LS-BASED POLYMERIC MATERIALS

## Objective

The objective is to evaluate the economic feasibility of converting NARA coproduct LS into functional polymeric materials with mechanical properties surpassing those of polystyrene, a standard techno-economic analysis was employed to estimate the production costs for the most promising LS-based plastics. The economic viability of replacing polystyrene (produced from petrochemical sources) was provisionally analyzed.

## Methodology

The production of lignosulfonate-based polymeric materials involves four major steps as shown in Figure LBP-3.1. The neutralized and ultrafiltered calcium lignosulfonate (Ca-LS) solution generated by the SPORL process will flow through an ion exchange vessel packed with Amberlite IR 120 H resin to protonate the sulfonate groups on the lignin macromolecules and remove metal cations present in the solution. The protonated lignosulfonate (H-LS) solution will be further concentrated through diafiltration. After spray-drying, the dried solid will be compounded and pelletized for injection-molding.

The neutralized SPORL spent liquor containing Ca-LS will be ultrafiltered through a 200 kDa molecular weight cut-off membrane to remove any solid residues, and the resulting permeate solution will be ultrafiltered through a 4 kDa molecular weight cut-off membrane to recover sugars (Zhu *et al.*, 2015). The retentate solution held by the 4 kDa membrane will be concentrated to 20 g/L. The resulting solution will be applied as the purified lignosulfonate solution in an ion exchange process. Such an ultrafiltration process, which maximizes the sugar yield, is crucial for biofuel production; therefore its cost will not be discussed in this report.

The batch of FS-01 Ca-LS was supplied by Dr. Junyong Zhu. It was used as the raw materials in this project. Since the purity and yield of FS-01 after ultrafiltration have not been determined, the purity of Ca-LS FS-10 after ultrafiltration (~90%), yield of FS-10 based on wood (~13%) (Zhu *et al.*, 2015) and its sulfur content ( $69.2 \pm 0.9$  mg/g of lignin) will be applied in the following cost estimation.

## Estimation of capital costs

In this section, the bare module cost for equipment (Turton *et al.*, 2012) will be applied to estimate the cost of a new chemical plant that is devoted to producing lignosulfonate-based polymeric materials (Table LBP-3.1). The bare module cost represents the sum of direct (equipment, materials required for installation, labor for installation) and indirect (freight, insurance, taxes, construction overhead and

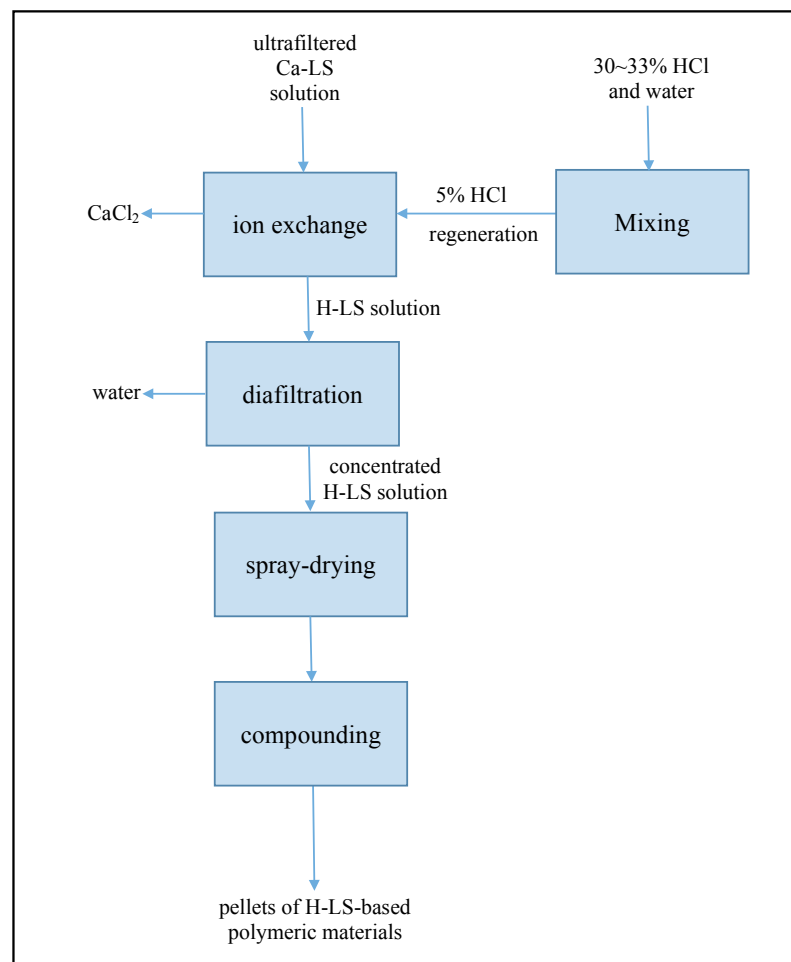


Figure LBP-3.1. A schematic process flow for producing lignosulfonate-based polymeric materials.

contractor engineering expenses) project expenses.

The equipment employed in each process block will be discussed in the following subsections. Along with their bare module costs, the corresponding total module cost and grass roots cost are summarized in Table LBP-3.1. Grass roots cost refers to the cost of establishing a completely new facility started on undeveloped land, and total module cost means the cost of making a small or moderate modification to an existing facility (Turton *et al.*, 2012).

### Ion exchange vessel

As shown in Figure LBP-3.1, the project is composed of 5 blocks. In the ion exchange block, the ion exchange resin will be packed in a vertical vessel (V-101) with 3.5 m diameter and 0.88 m height. Due to the low pH of the protonated lignosulfonate solution, the corrosion characteristics for materials of construction (MOC) for the vertical vessel have to be taken into consideration. Carbon steel subjected to anti-corrosion treatment will be used as the construction material for important equipment in this project. The resulting H-LS solution will be collected and stored in a 16 m<sup>3</sup> storage tank (TK-101) before diafiltration.

### Mixer

In the mixing process, the 30-33% HCl will be diluted 6-fold with water by using a turbine mixer (M-101). The resulting 5% HCl solution will be stored in a 16 m<sup>3</sup> storage tank (TK-102) before it is applied to resin regeneration.

### Equipment for diafiltration

The H-LS solution will be diafiltered through three tube filters (Fr-101, 102, 103) equipped with 4 kDa molecular weight cut-off membranes and pumps (P-101, 102, 103) to reduce solution volume 50-fold. The permeate solution containing a small amount of H-LS will be collected as wastewater in a 16 m<sup>3</sup> storage tank (TK-103).

### Spray-dryer

The concentrated retentate solution will be dried in a rotary spray-dryer (Dy-101), and then subjected to compounding (Z-101) for extruding and pelletizing. The energy usage of the spray-dryer will be calculated in section 3.4. Its utility cost (Table LBP-3.2) is estimated from the energy usage.

### Compounder

On the basis of the hourly production of H-LS listed in Table LBP-3.3, the purchase cost of the compounder can be referred to a HS TSE-95 compounding pelletizing machine model TSE-75B with capacity of 350-550 kg/h and motor power of 132 kW. Here, the bare module factor of the compounder is assumed to be 2.

Table LBP-3.1. Bare module cost for equipment estimated by CAPCOST computer program. The cost data has been adjusted for inflation on the basis of average Chemical Engineering's Plant Cost Index (CEPCI) in 2014 (576.1), (<http://www.chemengonline.com/economic-indicators-cepci/?printmode=1>)

Dryers	Type	Area (m <sup>2</sup> )		Purchased Equipment Cost	Bare Module Cost			
Dy-101	Rotary	5		\$ 29,200	\$ 36,500			
Filters	Type	Area (m <sup>2</sup> )		Purchased Equipment Cost	Bare Module Cost			
Fr-101	Tube	1		\$ 185,000	\$ 285,000			
Fr-102	Tube	1		\$ 185,000	\$ 285,000			
Fr-103	Tube	1		\$ 185,000	\$ 285,000			
Mixers	Type	Power (kW)		Purchased Equipment Cost	Bare Module Cost			
M-101	Turbine	15		\$ 14,200	\$ 19,500			
Pumps	Pump Type	Power (kW)	MOC	Discharge Pressure (barg)	Purchased Equipment Cost	Bare Module Cost		
P-101	Centrifugal	15	Carbon Steel	2	\$ 6,710	\$ 26,700		
P-102	Centrifugal	15	Carbon Steel	2	\$ 6,710	\$ 26,700		
P-103	Centrifugal	15	Carbon Steel	2	\$ 6,710	\$ 26,700		
Storage Tanks	Tank Type	Volume (m <sup>3</sup> )		Purchased Equipment Cost	Bare Module Cost			
Tk-101	Fixed Roof	16		\$ 61,400	\$ 67,500			
Tk-102	Fixed Roof	16		\$ 61,400	\$ 67,500			
Tk-103	Fixed Roof	16		\$ 61,400	\$ 67,500			
Vessels	Orientation	Height (m)	Diameter (m)	MOC	Demister MOC	Pressure (barg)	Purchased Equipment Cost	Bare Module Cost
V-101	Vertical	0.88	3.5	Carbon Steel	Flourocarbon	2	\$ 30,700	\$ 102,000
Compounders	Description	capacity (kg/h)	Actual BMF		Purchased Equipment Cost	Bare Module Cost		
Z-101	compounder	550	2		\$ 50,000	\$ 100,000		
<b>Total Bare Module Cost</b>						<b>\$ 1,295,600</b>		

Table LBP-3.2. The annual utility cost estimated by CAPCOST. The facility is assumed to operate 24 h a day for 345 days (8280 h). Daily Price of electricity (\$25.25/MWh) in Northwest in July 2016 was applied for utility cost estimation (<http://www.eia.gov/todayinenergy/prices.cfm>).

Name	Total Module Cost	Grass Roots Cost	Utility Used	Efficiency	Actual Usage	Annual Utility Cost
Dy-101	\$ 29,700	\$ 39,700	Electricity		13.4 kW	\$ 2,792
Fr-101	\$ 336,000	\$ 429,000	NA			\$
Fr-102	\$ 336,000	\$ 429,000	NA			\$
Fr-103	\$ 336,000	\$ 429,000	NA			\$
M-101	\$ 46,100	\$ 60,200	NA			\$
P-101	\$ 31,500	\$ 42,400	Electricity	0.7	21.4 kW	\$ 4,480
P-102	\$ 31,500	\$ 42,400	Electricity	0.7	21.4 kW	\$ 4,480
P-103	\$ 31,500	\$ 42,400	Electricity	0.7	21.4 kW	\$ 4,480
Tk-101	\$ 80,000	\$ 113,000	NA			\$
Tk-102	\$ 80,000	\$ 113,000	NA			\$
Tk-103	\$ 80,000	\$ 113,000	NA			\$
V-101	\$ 120,000	\$ 150,000	NA			\$
Z-101	\$ 59,000	\$ 109,000	Electricity		132 kW	\$ 27,580
<b>Totals</b>	<b>\$ 1,570,000</b>	<b>\$ 2,080,000</b>				<b>\$ 44,000</b>

Table LBP-3.3. Cost of Materials estimated by CAPCOST. The flowrates of materials are re-calculated on the basis of one cycle (6 h). The service life-time of Amberlite IR 120 H is assumed to be 7 years (Miller et. al., 2009)

Material Name	Classification	Price (\$/kg)	Flowrate (kg/h)	Annual Cost
Ca-LS	Raw Material	0	513.1	0
Amberlite IR 120	Raw Material	0.75	0.106	658
H-LS	Product	to be determined	471	
30~33% HCL	Raw Material	0.2	496	821,376
wastewater	Non-Hazardous Waste	0.000056	8851	4,104

## Results

### Cost of ion exchange

All the calculations are based on an ultrafiltered Ca-LS concentration of 20 g/L assuming that the density of the solution is 1 kg/L. Resin bed depth is 0.8 m taking into account resin swelling during service (as suggested by “Steps to Design an Ion Exchange Resin System”, <http://www.dow.com/en-us/water-and-process-solutions/resources/ion-exchange-resin-system>).

Material and energy balance on hourly basis for ion exchange process for one vessel is listed as follows:

- (1) Amberlite™ IR 120 H, Industrial Grade (Lenntech Water Treatment and Air Purification)
  - Bed volume (BV): 1 BV = 1 m<sup>3</sup> solution per m<sup>3</sup> resin
  - Shipping weight = 800 g/L
  - Volume =  $(3.5/2)^2 \times \pi \times 0.8 \times 1000 = 7696.9$  L
  - Weight =  $7696.9 \times 800/1000 = 6157.5$  kg
  - Total exchange capacity  $\geq 1.8$  eq/L = 90 g/L as CaCO<sub>3</sub>
  - Service flow rate = 5 BV/h
  - Regeneration flow rate = 1 BV/h for 2 h
  - Regeneration capacity per batch =  $90 \times 7696.9/1000 = 692.7$  kg as CaCO<sub>3</sub>
- (2) Ca-LS and H-LS
  - Concentration = 20 g/L
  - Ca-LS feeding rate during ion exchange operation =  $5 \text{ BV/h} = 7696.9 \times 5 \times 20/1000 = 769.7$  kg/h
  - Sulfur content = 69.2 mg/g lignin =  $69.2/32.065/1000 = 0.00216$  mol/g lignin
  - Ca<sup>2+</sup> concentration = 0.00216 mol/g lignin
  - Regeneration rate =  $0.00216 \times 100 \times 769.7 = 166.3$  kg/h as CaCO<sub>3</sub>
  - Hours of operation before regeneration =  $692.7/166.3 \approx 4$  h
  - Weight of H-LS =  $[769.7 - 769.7 \times 0.00216 \times (40.078 - 1.008 \times 2)] \times 4 = 2825.8$  kg (at 706.5 kg/h during operation period)
  - H-LS concentration =  $2825.8/(7696.9 \times 5 \times 4) = 0.01835$  kg/L

### Cost of mixing and resin regeneration

JB-B polypropylene anti-corrosive mixer with capacity of 400 L and mixing power of 1.5 kW is employed as reference for utility cost estimation (Table LBP-3.2). Usage of hydrochloric acid for resin regeneration is estimated according to the following equations:

$$5\% \text{ HCl flow rate} = 1 \text{ BV/h} = 7696.9 \text{ L/h}$$

$$\text{Hours of regeneration} = 2 \text{ h}$$

$$\text{Volume of 5\% HCl} = 7696.9 \times 2 = 15393.8 \text{ L}$$

$$\text{Density of 30~33\% HCl} = 1.16 \text{ g/cm}^3$$

$$\text{Volume of 30~33\% HCl} = 15393.8/6 = 2565.6 \text{ L} = 2565.6 \times 1.16 = 2976.1 \text{ kg}$$

$$\text{Water used for dilution} = 15393.8 - 2565.6 = 12828.2 \text{ L}$$

$$\text{Weight of CaCl}_2 = 0.00216 \times 769.7 \times 110.98 \times 4 = 738.0 \text{ kg}$$

Based on the material balance calculation, it can be assumed that each cycle of the ion exchange process will take 6 h in total for protonation and resin regeneration. The materials flow-rates listed in Table LBP-3.3 are estimated on the basis of one cycle of ion exchange. The daily production of H-LS for one ion exchange vessel will be approximately 11 tons. The facility is assumed to operate 24 h a day for 345 days (8280 h).

### Cost of diafiltration

The annual utility costs of three pumps are listed in Table LBP-3.2 assuming the pump efficiency is 0.7 and motor power is 21.4 kW. The materials balance in the diafiltration is estimated on the basis of one cycle (6 h) of the ion exchange process.

$$\text{Feed of H-LS solution} = 7696.9 \times 5 = 38484.5 \text{ L}$$

$$\text{Volume reduction factor} = 50$$

$$\text{Volume of H-LS solution after diafiltration} = 38484.5/50 = 769.7 \text{ L}$$

$$\text{Waste water (permeate)} = 769.7 \times 49 = 37715 \text{ L}$$

$$\text{H-LS concentration after diafiltration} = 0.01835 \times 50 = 0.92 \text{ kg/L}$$

$$\text{Weight of water in concentrated H-LS solution (assuming the density of 0.01835 kg/L H-LS equals to 1 kg/L)} = 38484.5 - 37715 - 0.01835 \times 38484.5 = 63.3 \text{ kg}$$

## Cost of spray-drying

The H-LS solution will be heated from 25°C to 75°C to evaporate the last trace of water. Assuming that the feed rate of H-LS for spray-drying equals the flow-rate of H-LS (471 kg/h, Table LBP-3.3), the hourly heat (Q) required to dry the concentrated H-LS solution from diafiltration can be estimated as follows:

Feed rate of water in concentrated H-LS solution for spray-drying =  $63.3/6 = 10.6$  kg/h

$Q = m_1 C_p DT + m_2 (C_{pw} DT + L) = 48.4$  MJ/h = 13.4 kilowatts

$m_1 = 471$  kg/h, the feed rate of H-LS

$m_2 = 10.6$  kg/h, the feed rate of water

$DT = 75 - 25 = 50^\circ\text{C}$

$C_p = 0.9148$  kJ/(kg·°C), heat capacity of H-LS at 25°C determined experimentally from DSC.

$C_{pw} = 4.180$  kJ/(kg·°C), heat capacity of water at 25°C

$L = 2322.8$  kJ/kg, heat of vaporization of water at 75°C

## Cost of compounding

In a continuous process for producing lignosulfonate-based polymeric materials, the feed rate of dried materials to the compounder is equal to the average flowrate of H-LS (471 kg/h, Table LBP-3.3). Therefore, the HS TSE-95 compounding pelletizing machine model TSE-75B with capacity of 350-550 kg/h and motor power of 132 kW will be a desirable reference for annual utility cost estimation (Table LBP-3.2).

## Cost of wastewater treatment

The wastewater stream listed in Table LBP-3.3 will be the combination of wastewater coming from regeneration of Amberlite resins and permeate solution from diafiltration (average wastewater flow rate =  $(37715 + 15393.8)/6 = 8851$  L/h). The main components in this wastewater stream will be  $\text{CaCl}_2$  and a small amount of H-LS. For tertiary wastewater treatment that involves filtration, activated sludge processing and chemical processing, it costs \$56 to treat 1000 m<sup>3</sup> of wastewater (Turton *et. al.*, 2012).

## Profitability Analysis

The profitability of this project is analyzed on the basis of a discontinued cash flow diagram. In the discontinued profitability model (Turton *et. al.*, 2012), the yearly cash flow is discontinued back to time zero; payback period is defined as the time required to recover the fixed capital investment ( $\text{FCI}_L$ , Table LBP-3.4); the net present value is defined as the cumulative discounted cash position at the end of the

project. It is assumed that the plant construction will take 2 years and the project will run for 15 years after the construction phase. Based upon the economic information listed in Table LBP-2.4, the cash flows as a function of H-LS selling price are compared in Figures LBP-3.2, 3.3 and 3.4 with  $\text{FCI}_L$  equal to grass roots cost, total module cost and 20% of grass roots cost, respectively.

When  $\text{FCI}_L = \text{Grass Roots Cost}$ , as summarized in Table LBP-3.5, the selling price of H-LS product cannot be set below \$0.7/kg, and \$0.8/kg is suggested to be a more appropriate price for a desired payback period (4.4 years) and a reasonable net present value (\$1.4 million) at the end of the project life. When the project is carried out in an existing facility with moderate modification to fit the equipment standards related to this project ( $\text{FCI}_L = \text{Total Module Cost}$ ), the selling price of H-LS can be reduced to \$0.75/kg to obtain a net present value around \$1.4 million in the 17th year (Figure LBP-3.3 and Table LBP-3.6). If  $\text{FCI}_L = 20\%$  of grass roots cost, then the price of H-LS will drop further to \$0.65/kg to secure a net present value of \$1.5 million.

Table LBP-3.4. Estimation of cost of manufacturing without depreciation ( $\text{COM}_d$ ) by CAPCOST. The revenue from sales is estimated based upon \$0.6/kg for H-LS selling price. Here,  $\text{FCI}_L$  equals Grass Roots Cost in Table LBP-3.2.

Economic Options		Factors Used in Calculation of Working Capital	
Cost of Land	\$ 50,000	Working Capital = $A \cdot C_{RM} + B \cdot \text{FCI}_L + C \cdot C_{OL}$	
Taxation Rate	42%	A	0.10
Annual Interest Rate	10%	B	0.10
Salvage Value	\$ 41,600	C	0.10
Working Capital	\$ 156,000	Project Life (Years after Startup) 15	
$\text{FCI}_L$	\$ 416,000	Construction period 2	
Total Module Factor	1.18		
Grass Roots Factor	0.50		
Economic Information Calculated From Given Information		Distribution of Fixed Capital Investment (must sum to one)	
Revenue From Sales	\$ 2,144,934	End of year One	60%
$C_{RM}$ (Raw Materials Costs)	\$ 822,034	End of year Two	40%
$C_{UT}$ (Cost of Utilities)	\$ 44,000	End of year Three	
$C_{WT}$ (Waste Treatment Costs)	\$ 4,104	End of year Four	
$C_{OL}$ (Cost of Operating Labor)	\$ 317,400	End of year Five	
Factors Used in Calculation of Cost of Manufacturing ( $\text{COM}_d$ )			
$\text{Comd} = 0.18 \cdot \text{FCI}_L + 2.76 \cdot C_{OL} + 1.23 \cdot (C_{UT} + C_{WT} + C_{RM})$			
Multiplying factor for $\text{FCI}_L$	0.18		
Multiplying factor for $C_{OL}$	2.76		
Factors for $C_{UT}$ , $C_{WT}$ , and $C_{RM}$	1.23		
$\text{COM}_d$	\$ 2,021,174		

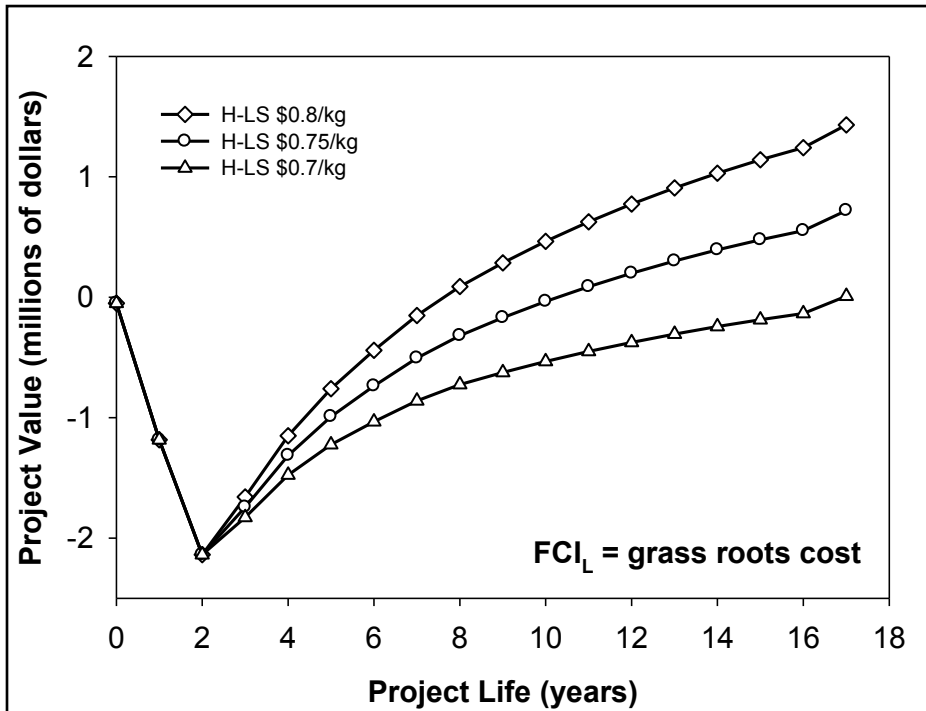


Figure LBP-3.2. Cumulative cash flow diagram for discounted after-tax cash flows as a function of H-LS selling price when  $FCI_L$  = Grass Roots Cost in Table LBP-3.2. The Modified accelerated cost recovery system (MACRS) depreciation is set to be 5 years.

Table LBP-3.5. Net present value, return rate and payback period for project as a function of H-LS selling price when  $FCI_L$  = Grass Roots Cost in Table LBP-3.2.

H-LS Price (\$/kg)	Net Present Value (millions of \$)	Return Rate	Payback Period (years)
0.8	1.43	20.2%	4.4
0.75	0.72	15.4%	6.0
0.7	0.01	10.1%	10.9

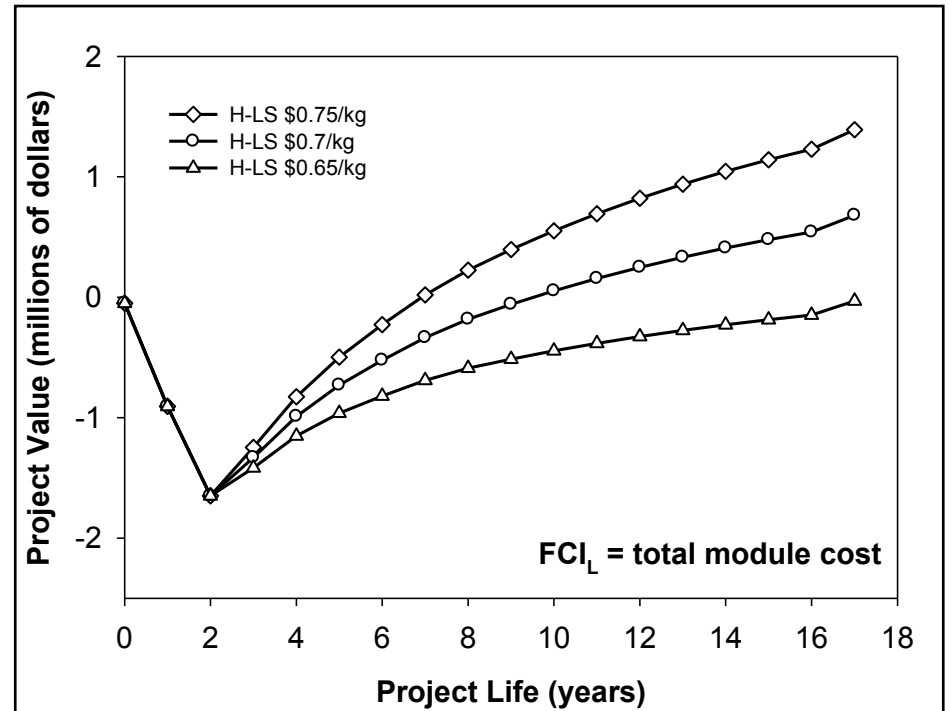


Figure LBP-3.3. Cumulative cash flow diagram for discounted after-tax cash flows as a function of H-LS selling price when  $FCI_L$  = Total Module Cost in Table LBP-3.2. The modified accelerated cost recovery system (MACRS) depreciation is set to be 5 years.

Table LBP-3.6. Net present value, return rate and payback period for project as a function of H-LS selling price when  $FCI_L$  = Total Module Cost in Table LBP-3.2.

H-LS Price (\$/kg)	Net Present Value (millions of \$)	Return Rate	Payback Period (years)
0.75	1.39	22.4%	3.8
0.7	0.68	16.5%	5.4
0.65	-0.03	9.7%	11.0

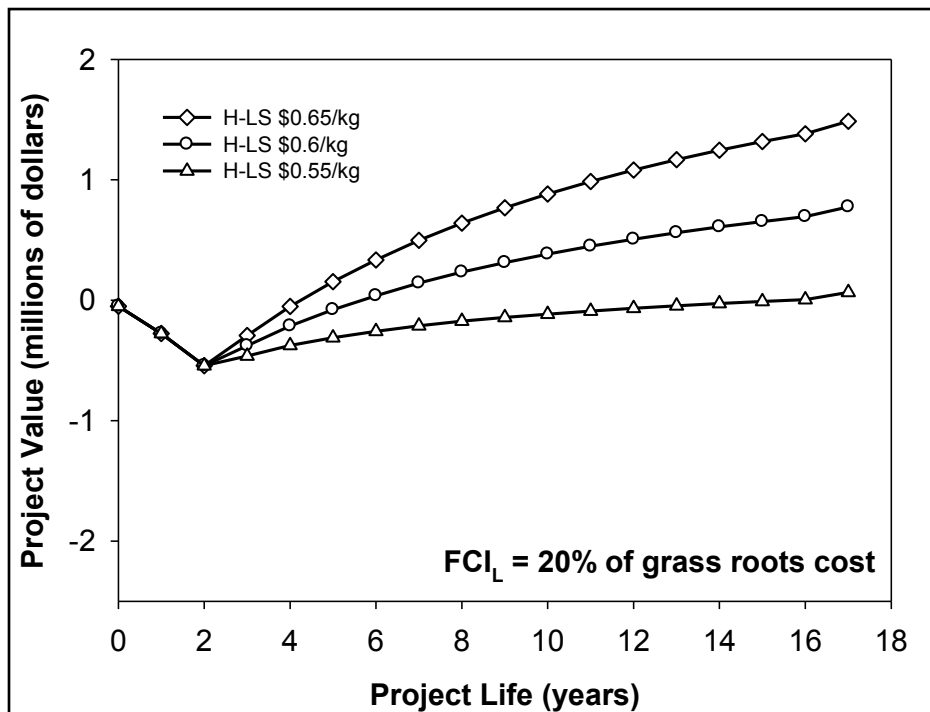


Figure LBP-3.4. Cumulative cash flow diagram for discounted after-tax cash flows as a function of H-LS selling price when  $FCI_L = 20\%$  of Grass Roots Cost in Table LBP-3.2. The Modified accelerated cost recovery system (MACRS) depreciation is set to be 5 years.

Table LBP-3.7. Net present value, return rate and payback period for project as a function of H-LS selling price when  $FCI_L = 20\%$  of Grass Roots Cost in Table LBP-3.2.

H-LS Price (\$/kg)	Net Present Value (millions of \$)	Return Rate	Payback Period (years)
0.65	1.49	42.1%	1.5
0.6	0.78	28.7%	2.3
0.55	0.07	11.9%	5.9

## Conclusions/Discussion

General purpose polystyrene was traded at around \$1,590/ton CFR (cost & freight) China in Asian market in May 2011 (<http://www.icis.com/resources/news/2007/11/06/9076435/polystyrene-ps-prices-and-pricing-information/>). The selling prices of H-LS estimated in this report are ~50% lower than that of polystyrene. Therefore, the NARA lignosulfonate obtained from the SPORL process could be viewed as a promising resource for producing future sustainable polymeric materials, and in return, improving the economic viability of the SPORL process to a great extent.

For better mechanical performance of the lignosulfonate-based polymeric

materials, some polyesters and polyols have been blended with H-LS at a 15% level to improve the ultimate tensile strength by ~50% and elongation at break ~2-fold (Wang *et al.*, 2015). The cost for producing lignosulfonate-based blends will increase correspondingly when 15% additional blend components are added. To secure ~\$1.5 million net present value for the project, the selling prices of the blends have to increase approximately by 40 cents/kg as shown in Table LBP-3.8, yet they are still lower than that of polystyrene.

The NARA LS obtained from the SPORL process could be viewed as a promising resource for producing future sustainable polymeric materials, and in return, improving the economic viability of the SPORL process overall. The implementation of LS-based polymer-blend production onto an industrial scale would greatly enhance the economic viability of converting lignocellulosic materials into liquid biofuels and commodity organic chemicals.

Table LBP-3.8. The selling price of lignosulfonate-based blends containing 15% polyester and polyols. The market price for blend components was assessed at \$2.60-3.26/kg in 2014 (<http://www.icis.com/resources/news/2014/05/28/9785895/polyester-polyols-6-cent-lb-hike-proposed-on-rising-costs/>).

$FCI_L$	Price (\$/kg)	Net Present Value (millions of \$)	Return Rate	Payback Period (years)
Grass Roots Cost	1.17	1.49	19.8%	4.2
Total Module Cost	1.13	1.49	22.1%	3.5
20% of Grass Roots Cost	1.04	1.50	36.9%	1.4

The first techno-economic analysis of NARA LS-based plastics is very encouraging. For better mechanical performance of the NARA LS-based polymeric materials, some polyesters have been blended at a 15 wt% level to improve the ultimate tensile strength by ~50% and elongation-at-break ~2-fold (Wang *et al.*, 2015). Even with the increase in expenses for additional blend components, the costs for producing NARA LS-based blends as engineering plastics are still lower than that of polystyrene.

# NARA OUTPUTS

## Patents

Compositions Including Ligninsulfonate, Compositions Including Un-alkylated Lignin, and Methods of Forming: Chen, Y.-r.; Sarkanen, S.; Wang, Y.-Y. **2015**, Provisional Patent Application No. 62/215,017, September 6.

Compositions Including Lignin: Chen, Y.-r.; Sarkanen, S.; Wang, Y.-Y. **2015**, International Patent Application No. PCT/US2015/020599, filed March 13.

Compositions Including Lignin: Chen, Y.-r.; Sarkanen, S.; Wang, Y.-Y. **2014**, U.S. Provisional Patent Application No. 61/953,118 filed March 14.

## Presentations

S. Sarkanen, Y.-r. Chen, Y.-Y. Wang. Formulations for Coproduct Lignin-based Plastics. Oral presentation at NARA Coproducts Team Meeting, Spokane, WA, August 22, 2012.

Y.-Y. Wang, S. Sarkanen, Y.-r. Chen. Formulations for Coproduct Lignin-based Plastics. Oral presentation at NARA 2012 Annual Meeting, Missoula, MT, Sept 13-14, 2012.

Y.-Y. Wang, S. Sarkanen, Y.-r. Chen. Formulations for Coproduct Lignin-based Plastics. Poster presentation at NARA 2012 Annual Meeting, Missoula, MT, Sept 13-14, 2012.

S. Sarkanen, Y.-r. Chen, Y.-Y. Wang. Formulations for Coproduct Lignin-based Plastics. Oral presentation at NARA Coproducts Team February 2013 Quarterly Meeting, Spokane, WA, February 27, 2013.

S. Sarkanen, Y.-r. Chen, Y.-Y. Wang. Formulations for Coproduct Lignin-based Plastics. Oral presentation at NARA Coproducts Team Meeting, Spokane, WA, March 5, 2014.

Y.-r. Chen, S. Sarkanen, Y.-Y. Wang. Through Lignin Depolymerase to Native Lignin-based Plastics. Oral presentation at 247th American Chemical Society National Meeting, Dallas, TX, March 16-20, 2014.

S. Sarkanen, Y.-r. Chen, Y.-Y. Wang. Formulations for Coproduct Lignin-based Plastics. Oral presentation at NARA Coproducts Team Meeting, Spokane, WA, November 14, 2013.

S. Sarkanen, Y.-Y. Wang, Y.-r. Chen. Prospects for Lignin-based Plastics from Biorefineries. Invited (all expenses paid) Oral presentation at Lignin 2014 Conference in Sweden, August 24 – 28, 2014.

S. Sarkanen, Y.-Y. Wang, Y.-r. Chen. Lignin-based Plastics from Biorefineries. Invited Oral presentation at VTT Technical Research Centre of Finland, September 3, 2014.

S. Sarkanen, Y.-Y. Wang, Y.-r. Chen. Highest Attainable Lignin Contents in Polymer Materials from Biorefineries. Keynote Oral presentation at Lignobiotech III Symposium, Concepción, Chile, October 26-29, 2014.

Y.-Y. Wang, Y.-r. Chen, S. Sarkanen. Macromolecular Characterization of Plastics with 85-100% Levels of Methylated Native Softwood Lignin." at 249th American Chemical Society National Meeting, Denver, Colorado, March 22 – 26, 2015.

S. Sarkanen, Y.-Y. Wang, Y.-r. Chen. Plastics containing unprecedented 85-100% levels of methylated softwood lignin compare favourably with polystyrene. Oral Presentation at the 11th International Conference on Renewable Resources & Biorefineries, York, England, June 3-5, 2015.

Y.-Y. Wang, S. Sarkanen, Y.-r. Chen. Plastics with the highest native lignin contents are nano-biomaterials composed of 13 nm macromolecular complexes. Oral Presentation at 2015 TAPPI International Conference on Nanotechnology for Renewable Materials, Atlanta, GA, June 22 – 25, 2015.

S. Sarkanen, Y.-Y. Wang, Y.-r. Chen. Formulations for Coproduct Lignin-based Plastics. Oral Presentation at NARA Coproducts Team Meeting, Pullman, WA, July 22, 2015.

Y.-Y. Wang, Y.-r. Chen, S. Sarkanen. NARA Ligninsulfonate-based Plastics. Poster presentation at the Northwest Advanced Renewables Alliance Annual Meeting, Spokane, WA, September 2015.

Y.-Y. Wang, Y.-r. Chen, S. Sarkanen. Useful Plastics with Very High Lignin Contents Should be Imminent." PacifiChem 2015, Honolulu, HI, December 15 – 20, 2015.

Y.-Y. Wang, Y.-r. Chen, S. Sarkanen. Journey to Polymeric Materials Composed Exclusively of Simple Lignin Derivatives." Oral Presentation at 251st American Chemical Society National Meeting, San Diego, California, March 13 – 17, 2016.

Y.-r. Chen, Y.-Y. Wang, S. Sarkanen. To Methylate or Not To Methylate Polymeric Materials with the Highest Attainable Lignin Contents." Oral Presentation at 251st American Chemical Society National Meeting, San Diego, California, March 13 – 17, 2016.

S. Sarkanen, Y.-Y. Wang, Y.-r. Chen. Functional Polymeric Materials with the Highest Levels of Softwood Lignin and Ligninsulphonates. Oral Presentation at 12th International Conference on Renewable Resources and Biorefineries, Ghent, Belgium, May 30 – June 1, 2016.

Y.-Y. Wang, Y.-r. Chen, S. Sarkanen. Plastics with 85-100% Levels of Lignin from Softwoods and Wheat straw." Oral Presentation at 4th Symposium on Biotechnology applied to Lignocelluloses (LignoBiotech IV), Madrid, Spain, June 19 – 22, 2016.

## Publications

Sarkanen, S., Wang, Y.-Y., Chen, Y.-r. Plastics composed entirely of methylated ball-milled lignins and ligninsulfonates. *18th Internat. Symp. Wood Fibre Pulp. Chem.* 2015, Vol. 1, 93-95.

Wang, Y.-Y., Chen, Y.-r., Sarkanen, S.: Path to plastics composed of ligninsulphonates (lignosulfonates). *Green Chemistry* 2015, 17, 5069-5078.

Wang, Y.-Y., Chen, Y.-r., Sarkanen, S.: Plastics composed of a simple lignin derivative alone and nearby blends. *Biomacromolecules*, under review.

Sarkanen, S., Chen, Y.-r., Wang, Y.-Y.: Journey to polymeric materials composed exclusively of simple lignin derivatives. *ACS Sustainable Chemistry & Engineering*, submitted.

# NARA OUTCOMES

---

- A 40 wt% incorporation limit for lignin in polymeric materials that was typically encountered for the past 40 years has been overcome by our discovery that polymeric materials composed of 85–100 wt% (native) ball-milled softwood lignin possess mechanical properties surpassing those of polystyrene.
- Underivatized Douglas-fir NARA LS blended with small quantities (<15 wt%) commercially available aliphatic polyesters can engender polymeric materials with mechanical properties better than those of polystyrene.
- The mechanical properties of these novel NARA LS-based polymeric materials can be effectively modulated by other blend components.
- These new materials are composed of associated macromolecular complexes with ~12 nm dimensions.
- Techno-economic analysis shows that, upon optimization, NARA LS-based polymeric materials could become viable alternatives as biodegradable plastics to polystyrene produced from petrochemical sources.

# FUTURE DEVELOPMENT

---

Systematic approaches should be devised to identify plasticizers for developing functional polymeric materials with the highest attainable ligninsulfonate contents. Industrial conditions adopted by the private sector to derivatize ligninsulfonates for incorporation into plastics formulations will be a centrally important step for bringing LS-based polymeric material into the market place.

# LIST OF REFERENCES

- Chen, Y.-r. & Sarkanen, S. (2006). From the macromolecular behavior of lignin components to the mechanical properties of lignin-based plastics. *Cellulose Chem. Technol*, 40, 149-163, and references therein.
- Chen, Y.-r. & Sarkanen, S. (2010). Macromolecular replication during lignin biosynthesis. *Phytochemistry* 71, 453-462.
- Hsu, O.H.-H. & Glasser, W.G. (1976). Polyurethane adhesives and coatings from modified lignin. *Wood Sci.*, 9, 97-103.
- Miller, W. S., Castagna, C. J., & Pieper, A. W., (2009, June) Understanding Ion-exchange Resins For Water Treatment Systems, GE Water & Process Technologies.
- Li, Y. & Sarkanen, S. (2002). Alkylated kraft lignin based thermoplastic blends with aliphatic polyesters. *Macromolecules*, 35, 9707-9715.
- Li, Y. & Sarkanen, S. (2005). Miscible blends of kraft lignin derivatives with low- $T_g$  polymers. *Macromolecules*, 38, 2296-2306.
- Saito, T., Brown, R. H., Hunt, M. A., Pickel, D. L., Pickel, J. M., Messman, J. M., Baker, F. S., Keller, M. & Naskar, A. K. (2012). Turning renewable resources into value-added polymer: development of lignin-based thermoplastic. *Green Chem.*, 14, 3295-3303.
- Saito, T., Perkins, J. H., Jackson, D. C., Trammel, N. E., Hunt, M. A. & Naskar, A. K. (2013). Development of lignin-based polyurethane thermoplastics. *RSC Adv.*, 3, 21832-21840.
- Turton, R., Bailie, R. C., Whiting, W. B., Shaeiwitz, J. & Bhattacharyya, A., D. (2012). *Analysis, Synthesis and Design of Chemical Processes*. 4<sup>th</sup> edition, Pearson Education, Inc., Upper Saddle River, NJ.
- U.S. Department of Energy. (2006). *Breaking the Biological Barriers to Cellulosic Ethanol: A Joint Research Agenda*, DOE/SC-0095, U.S. Department of Energy Science and Office of Energy Efficiency and Renewable Energy Washington, D.C., pg. 205. Retrieved from <http://genomicsgtl.energy.gov/biofuels/2005workshop/b2blowres63006.pdf>.
- Wang, Y.-Y., Chen, Y.-r. & Sarkanen, S. (2015). Path to plastics composed of ligninsulfonates (lignosulfonates), *Green Chem.*, 17, 5069-5078.
- Zhu, J.Y., Chandra, M. S., Gu, F., Gleisner, R., Reiner, R., Sessions, J., Marrs, G., Gao, J. & Anderson, D. (2015). Using sulfite chemistry for robust bioconversion of Douglas-fir forest residue to bioethanol at high titer and lignosulfonate: A pilot-scale evaluation. *Bioresour. Technol.*, 179, 390-397.